Research Paper

Evaluation of Asphalt Mixtures From the Correction of the Failure Area in the IDEAL Test

Oscar Javier REYES-ORTIZ*, Juan Sebastian USECHE-CASTELBLANCO, Marcela MEJIA

Universidad Militar Nueva Granada
Bogota D.C., Colombia
e-mail: 7700125@unimilitar.edu.co; angela.mejia@unimilitar.edu.co
*Corresponding Author e-mail: oscar.reyes@unimilitar.edu.co

The IDEAL cracking test was developed in 2019 in the Texas A&M Transportation Institute as an alternative to evaluate the fracture tolerance of asphalt mixtures by the same indirect tensile strength test but with a different interpretation. In this methodology, the fracture area is described as a plane surface. However, the fracture of the asphalt mix is characterized by its irregularity and a non-uniform failure surface. For this reason, this work presents a model to determine the actual area of the failure for a set of asphalt mixtures with different characteristics using a 3D scanner. The main goal is to determine a possible correction factor of the actual fracture surface and observe the IDEAL test modification. This study shows that it is possible to standardize the correction factor for four of the five mixtures.

Key words: IDEAL test; 3D scanner; fracture resistance, asphalt mixtures.

1. Introduction

Cracking in asphalt mixtures is one of the most common failures that occur in a pavement structure, either due to its use (application of loads) or to the environmental conditions to which it has been subjected [1, 2]. In this context, multiple tests have been developed for the analysis of the fracture resistance of an asphalt mixture. These tests allow to create design models and build more resistant and durable pavement structures. Among the tests, there are the semi-circular bending test (SCB), the Fénix test, the indirect tensile strength test (IDT), and the resilient module test. However, recent studies [3] have proposed the IDEAL test as an alternative.

The importance of fracture resistance analysis is reflected in recent research, including the work of XUAN *et al.* [4]. The authors, using the SCB test, analyzed the fracture resistance of mixtures with high reclaimed asphalt pavement (RAP) contents, and observed that when adding additives, it is more efficient to make addition directly to aggregate instead of modifying the binder first. ZIARI and

Moniri [5] determined the mechanical and dynamic response of modified asphalt mixtures with synthetic fibers. The researchers evaluated their response from the load vs. displacement curve to establish that the fibers improve resistance to moisture damage and fatigue. Pérez *et al.* [6] analyzed the fracture resistance of asphalt mixtures by evaluating the SCB and Fénix tests. The authors presented a comparative analysis of the tests where it is observed that both tests show the same behavior in the calculation of the rigidity index and dissipated energy (indicators of fracture resistance). Additionally, Mahyuddin *et al.* [7] applied the indirect tensile strength test to analyze the stability of asphalt mixtures with natural asphalt binder (i.e., composition consisting of 27% asphalt binder and 63% granular material); the procedure was based on the load vs. displacement curve and they took the maximum point to perform the analysis. It was reported that with an increase in natural asphalt binder content from 2.5% to 7.5%, the IDT value increased by approximately 9%.

The previous tests individually present advantages, but at the same time deficiencies in their methodology. For example, the IDT test within its analysis model does not take into account the total area of the load vs. displacement curve, and the evaluation of fracture tolerance is done indirectly [8]. Reyes *et al.* [9] concluded that the parameter corresponding to the area under the curve refers to the energy dissipated by the specimen during the IDT test and it is fundamental to characterize its resistance to fracture. Due to the importance of studying this characteristic, the need to implement a test that combines the advantages of present methodologies as an alternative to initiate new design models was created [10].

In this context, the IDEAL test emerged in the United States at the beginning of 2019, funded by the NCHRP IDEA program that seeks to develop new methodologies for the design, construction, and maintenance of roads. This program has been funded by AASHTO, searching for innovative methods to improve the safety and behavior of roads and highways [11]. The IDEAL test developed by the Texas A&M Transportation Institute is an adaptation of the IDT test, but it expands in its analysis and understanding. The IDEAL test procedure consists of the complete acquisition of the load vs. displacement curve (LvsDC) and the distinction of four regions within the curve. The segmented regions are shown in Fig. 1. The load application speed (50 mm/min) and the execution temperature (25°C) are standardized. Then, applying a method of analysis on the third region of the curve, the fracture tolerance index (CT_{Index}) is obtained that refers to the resistance of the structure after the failure occurs. This allows to know its capacity to dissipate energy while the crack propagates. Within the development of the IDEAL test, the CT_{Index} shows a correlation with different laboratory tests that focus on the cracking study, as in the case of fatigue cracking or reflective cracking, among other laboratory tests [3].
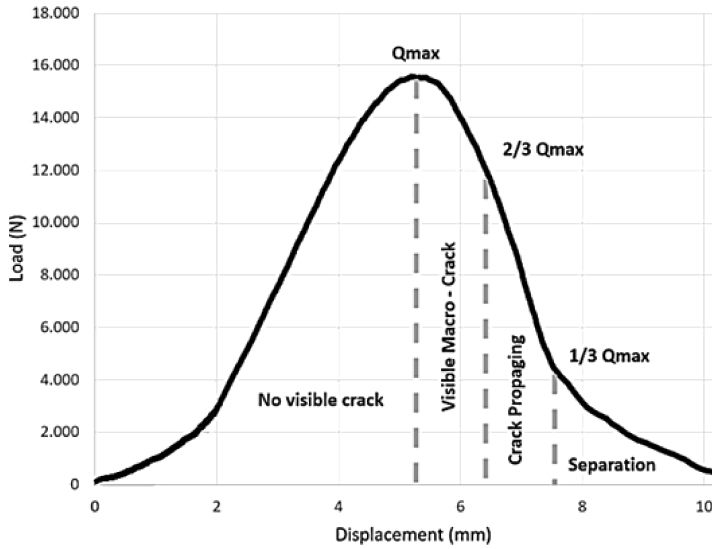
Fig. 1. Segmentation of the LvsDC of the indirect tensile strength test.

The methods of analysis of the laboratory tests (including the IDEAL test) present generalities in their methodology, which standardize some parameters that change drastically depending on the kind of mixture [12]. This is because the structural components of an asphalt mix have a heterogeneous behavior depending on their geological origin, the environmental conditions to which the pavement is subjected, their use conditions, and the type of mix designed according to each national standard [13, 14]. An example of the above is presented in the IDEAL test, where the equations establish the fracture area as a plane calculated by the multiplication of the diameter and height [3]. The actual fracture area and the crack's propagation vary completely from one type of mixture to another. In this way, due to the standardization of the failure area, the behavior and resistance of some types of mixtures can be overestimated [15, 16].

In recent years, some researchers have studied the characterization of the fissures' shape and propagation, such as the study by WANG et al. [17]. Using a finite element algorithm in 2D, the authors characterized the crack generated in the SCB test to determine the crack initiation angle, the location, and its propagation route. The authors determined that the crack propagates by points of specific stresses related to the distribution of the aggregate and its form [17]. STEWART and GARCÍA [18] implemented a 3D scanning system to track the crack propagation for different types of mixtures tested by indirect traction. The authors noted that in a high percentage, the crack propagates through the mastic, avoiding the aggregate and creating a fractured irregular surface [18]. ESPINOSA et al. [19] presented an acquisition model to the area of the fractured

surface, where they calculated the area of failure and compared it with the square area of the specimens after applying the SCB test. The authors concluded that using the plane area to perform the calculations is a valid approximation, though it is possible to overestimate the fracture energy.

Although there are investigations that attempt to analyze the shape of the crack and the failure surface area of different types of asphalt mixtures, there is no a correction factor presented to be used in the laboratory. Additionally, the methods used for scanning the fracture area are complex and expensive.

This research presents the results of a simple process of fracture area correction for different types of asphalt mixtures (a recycled asphalt mixture with 70% RAP-recycled asphalt concrete, mixtures with asphaltite-natural asphalt binder manufactured in cold and hot, a dense asphalt mixture and a draining mixture) and its impact on the CT_{Index} value calculation of the IDEAL test. For the area correction model, a 3D acquisition system is implemented that allows digitizing the fracture area in its actual measurements. Subsequently, a correction factor of the failure surface is obtained for each of the mixtures, observing their regularity to determine if standardization of the factor is possible. This paper is divided into the 'methods and materials' section, which shows the manufacturing process, the implementation of the test based on what was presented by ZHOU [3] in the final report of the NCHRP IDEA 195 project, the surface acquisition, and finally, the area correction model. Then the results are evaluated and analyzed to conclude.

2. METHODS AND MATERIALS

The methodology for the development of the research is presented in Fig. 2. It begins with the characterization of asphalt binder, aggregates, RAP, and as-
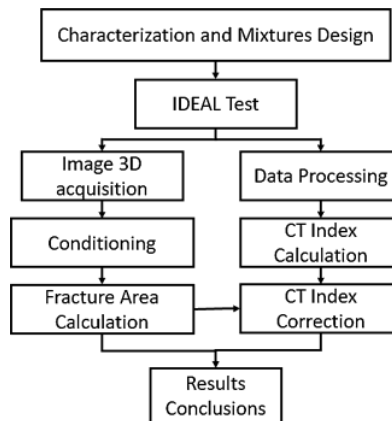

FIG. 2. Work methodology.

phaltite. Subsequently, the mix design is established for each of the materials to be used. Then, the manufacturing process of the specimens and the application of the IDEAL test are made. After the process of acquiring the actual failure surface, the correction of the test is done, and with the results the correction factor for the different types of asphalt mixtures is determined.

2.1. Characterization of materials and design of mixtures

In the development of the research project, the stone aggregates were characterized by laboratory tests standardized in international regulations (American Society for Testing and Materials, British Standards, and by the European Committee for Standardization), and the results are presented in Table 1. A 60–70.1 mm penetration bitumen is used [20]. The natural asphalt binder used (asphaltite) corresponds to a deposit of sand saturated with water and a naturally refined asphalt binder, located in southern Colombia, with an asphalt binder content of 8% [21]. The fraction of RAP used is coarse material inside the sieves of $1/2''$ to $3/8''$ and fine material between No. 40 and No. 200 sieve.

Table 1. Characterization of the aggregate.

Parameter	Standard	Result
Bulk density, S [g/cm3]	ASTM C 128 – 07a	2.68
Nominal density [g/cm3]	ASTM C 128 – 07a	2.55
Bulk density S.S.S. [g/cm3]	ASTM C 128 – 07a	2.60
Absorption [%]	ASTM C 128 – 07a	2.0
Los Angeles machine [%]	ASTM C 131 – 06	24.19
Sand equivalent [%]	ASTM D 2419 – 09	59
Flattening Index [%]	BS 812-105.1:1989	14.6
Elongation Index [%]	BS 812-105.2:1990	17.6
Percentage of fractured faces [%]	ASTM D 5821 – 01	92.2/90.1
Methylene blue g/1000 g	EN 933 – 9	0.3
Consistency limits [plastic, liquid] and plasticity index [%]	ASTM D 4318 – 10	No plastic
Sulfate Resistance Test [%]	ASTM C 88 – 05	10.0
Material passes sieve # 200 [%]	ASTM C 117 – 04	4.1

To manufacture the different asphalt mixtures, the sieve curves stipulated in the technical specifications of INVIAS were used [20] (see Fig. 3):

- Recycled mixture: MDC-19 sieve curve, Mix code: MDC-19-RAP. For this mixture, an MDC-19 sieve curve was used with a modification in the medium sieves where virgin material was included. In this way, an asphalt mix with 70% RAP was manufactured.
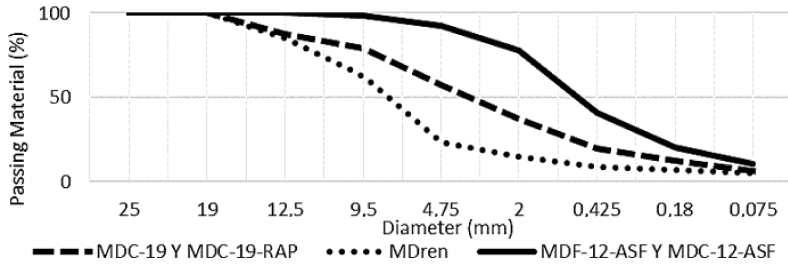
Fig. 3. Sieve curves.

- Cold asphaltite mixture: MDF-12 sieve curve, Mix code: MDF-12-ASF.
- Hot asphaltite mixture: MDF-12 sieve curve, Mix code: MDC-12-ASF.
- Hot dense mixture: MDC-19 sieve curve, Mix code: MDC-19.
- Draining mixture: the sieve curve is indicated in article 453-INVIAS [18], Mix code: MDren.

2.2. *Manufacture of asphalt mixtures*

To avoid problems of thermal segregation or mixing differentials, a mixer with controlled revolutions and temperature was used (Fig. 4). To manufacture the specimens the gyratory compactor was used, reaching an average of air voids of 4.8% in the MDC-19-RAP mixture, 4.2% in the MDF-12-ASF – MDC-12-ASF, 5% in the MDC-19 mixture and 20% in the MDren. The specimens used are Marshall type, following the recommendation of the geometrical characteristics for the IDEAL test [3].

Fig. 4. Manufacture of asphalt mixtures.

2.3. IDEAL test execution

The test equipment is presented in Fig. 5, which applies controlled movement and measures the applied load in real-time. The equipment also consists of a temperature chamber with which the samples are conditioned for 24 hours. The IDEAL methodology [3] uses the same procedure of the indirect tensile strength test with a load application speed of 50 mm/min and measuring the vertical displacement in the load direction. Additionally, for the implementation of the test, the capture of the complete LvsDC is necessary. The test suggests a conditioning temperature of 25°C, but in this investigation, it was performed at 15°C to simulate the characteristic temperature of multiple regions of the study site.

FIG. 5. IDEAL test.

In the IDEAL test, the LvsDC is divided into four regions: where the fissure is not visible, where the fissure begins to be observed, where the fissure propagates at high speed, and where the specimen is divided into two pieces. The four phases occur over seven moments that can be distinguished in the curve obtained and are described in Table 2.

The main objective of the analysis performed in the IDEAL test is to calculate the CT_{Index} that refers to the fracture tolerance index. The higher this index is the better is the tolerance to cracking of the specimen. To obtain this value, the analysis region was defined after the maximum load point, since in this region it is possible to analyze both the behavior and the propagation of the crack along the asphalt mix [3]. Based on the above, Eq. (2.1) is established [22, 23]

$$(2.1) \qquad CT_{\text{Index}} = \frac{h}{62} \cdot \frac{G_f}{|m_{75}|} \cdot \frac{l_{75}}{D},$$

where h and D are the height and diameter of the specimen, respectively, G_f is the fracture work (area of the LvsDC divided by the area of the fracture face),

Table 2. Regions of the LvsDC [3].

Region	Phase	Range	Region in test sample
Pre-peak load	1	0 to $\frac{1}{3}Q_{\max}$. Start of load increase	No visible crack
	2	$\frac{1}{3}Q_{\max}$ to $\frac{2}{3}Q_{\max}$. Accelerated load increase	
	3	$\frac{2}{3}Q_{\max}$ to $Q_{\max}$. Decreased rate of load increase	
Peak load	4	$Q_{\max}$. Peak load point	
Post-peak load	5	$Q_{\max}$ to $\frac{2}{3}Q_{\max}$. Load decreasing	Starting to see visible macro-crack
	6	$\frac{2}{3}Q_{\max}$ to $\frac{1}{3}Q_{\max}$. Load decreasing	Crack propagating quickly
	7	$\frac{1}{3}Q_{\max}$ to 0. Load decreasing	Specimen separation

and m_{75} and l_{75} are the slope and the load at 75% of the maximum load after failure according to ZHOU [3]. At this point, the test has the maximum speed of propagation of the crack and, therefore, the characteristic point to determine the fracture tolerance. The parameter units of length and load in Eq. (2.1) are expressed in millimeters and Newtons, respectively. In the research, the objective is to correct the fracture work G_f which is obtained using the final area of failure.

2.4. Capture and processing of the fracture area

As it can be seen in Fig. 5, the area of failure is not rectangular. To obtain the actual area, a capture protocol is initiated using the Kinect® depth sensor. This sensor allows to measure different objects that are within a region of space. The acquisition space is shown in Fig. 6, where the distribution of the elements
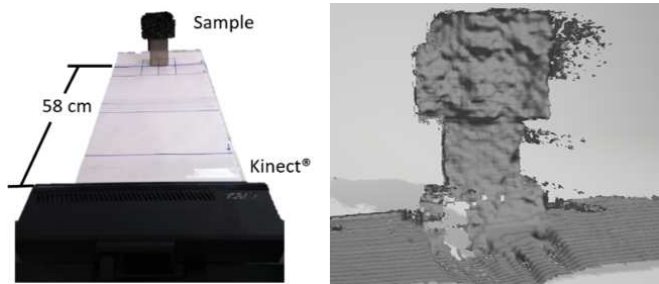

FIG. 6. Set and acquisition interface.

is presented. The depth sensor of the device by default is configured with low sensitivity to external light disturbances, which simplifies the assembly, capture and is easy to apply.

For the acquisition of the fractured area, the application of the Kinect SDK environment for Windows® of free access is used. The scanning region is configured to acquire the surface of the asphalt sample with as many points as possible. The acquisition of the solid conserves the real lengths of the element in millimeters and the final surface has 20 000 triangular faces (Tf) on average. With the above, a resolution of 3 Tf/mm^2 is obtained using the mean value of the height and diameter of the specimens. In other words, every square millimeter of the fracture surface is reconstructed by three triangles. Figure 7 shows the resulting surface for an MDC-19 sample.
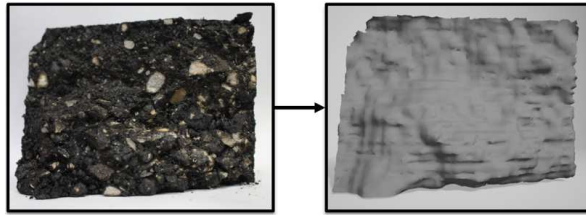

FIG. 7. An MDC-19 surface extraction.

2.5. Area calculation

To calculate the area, the surface of one sample is imported into Matlab® as illustrated in Fig. 8, where a mesh of vertices and faces with real dimensions is obtained. Then each area triangle of vertices (x, y, z) is calculated and a summation is applied to obtain the surface total area. The z-axis measures the depths over the failure plane. With this new area, the value CT_{Index} is corrected for each sample to make the comparison.
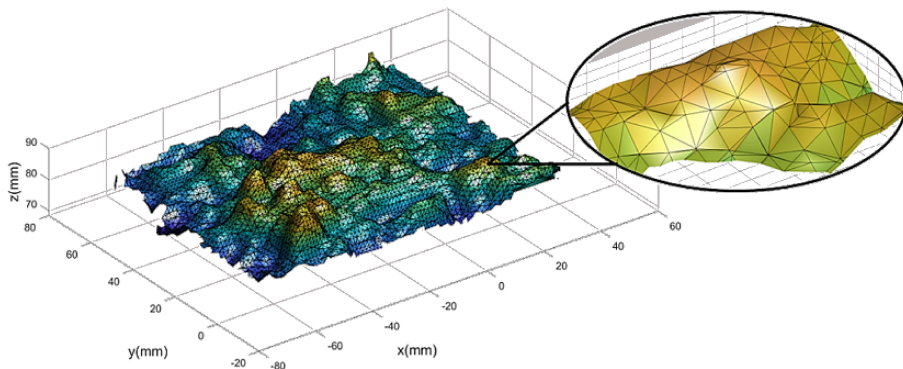

FIG. 8. Surface import.

3. Result analysis

Figure 9 shows the load vs. displacement curves for the indirect tensile test performed on ten specimens of each type of asphalt mixture evaluated. These re-
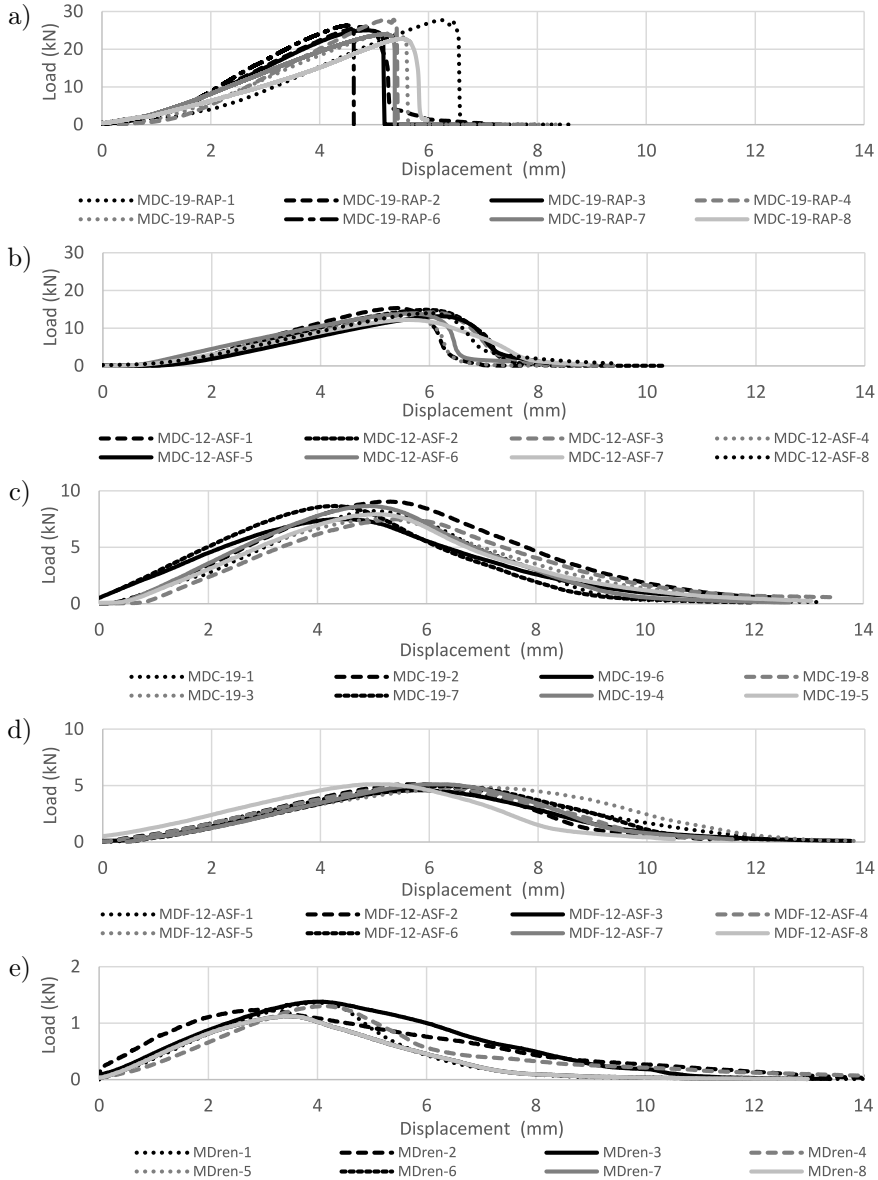

Fig. 9. LvsDC for asphalt mixes: a) recycled mix (MDC-19-RAP),
b) hot asphaltite mix (MDC-12-ASF), c) dense mix (MDC-19),
d) cold asphaltite mix (MDF-12-ASF), and e) draining mix (MDren).

sults allow to distinguish clearly the differential resistance of the mixtures, some being more rigid or ductile than others. These characteristics are fundamental to differentiate the response to fracture of the mixtures studied.

In the data presented in Fig. 9a, there is a coincidence with the observations made by ZHOU [3]. Zhou indicated problems in the calculation of the CT_{Index} in mixtures of high rigidity, such as those with recycled material (RAP). This can be related to the fact that the displacement of the curve after the maximum load is practically vertical and the slope (m_{75}) can even be undetermined. In the draining mixture, the low slopes of the curve after the maximum load, are associated with high air void content and a lower number of contact points in the granular skeleton (compared to the dense mixtures). Although the draining mixture is used as a functional layer, the characterization of its fracture tolerance is still of interest to deepen understanding of the "raveling" phenomenon that affects these mixtures [24].

With each of the LvsDC, the CT_{Index} is obtained per test sample. Subsequently, the mean is calculated by the type of mixture, and the respective values are presented in Fig. 10. It is observed how the cold asphaltite mixture has better tolerance to cracking compared to the recycled mixture (MDC-19-RAP). The mixture MDF-12-ASF and the mixture MDREN present high values of tolerance against cracking even with small maximum loads, and an explanation can be that the values of their slopes $|m_{75}|$ were low. The above can be observed in Fig. 9 for all mixes. After the maximum load, the curve for these two kinds of mixtures descends slowly, manifesting higher ductility. In MDC-19-RAP and MDC-12-ASF mixtures, the accelerated descent of the curves is observed. Although their fracture energy is high, when it is divided by high slopes, the results are reduced factors. In the MDC-19 mixture, greater stability is observed between the fracture energy (area under the curve) and the slope of descent, making a good relationship between them and, therefore, a better result is obtained. On the other hand, in Fig. 10 the coefficient of variation (COV – standard deviation divided by the mean) for the CT_{Index} of each of the mixtures is also presented.
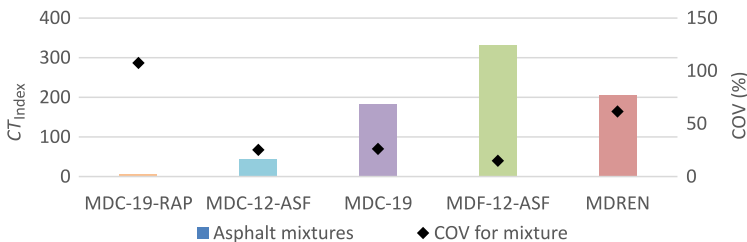

FIG. 10. CT_{Index} for asphalt mixtures and coefficient of variation.

It is necessary to note that ZHOU [3] evaluated specimens with 15 and 20% RAP content, in which the CT_{Index} was low with values of 40 and 30 respectively, but calculable with a coefficient of variation per mixture of 20. With the experiment performed at 15°C, it is observed that for a mixture of 70% of RAP, the value of the CT_{Index} is not calculable, although on average a value of 5 is obtained, the COV is over 100%. This is because CT_{Index} values vary from 1 to 13. From these results, it is observed that the cracking tolerance index presents an acceptable variability for the evaluation of conventional dense mixture and mixtures made with asphaltite. However, the recycled and draining mixture has high variability, which suggests the need for further research to improve the characterization of these two kinds of mixtures through the IDEAL test for the conditions suggested in this work.

In the case of mixtures with recycled material (MDC-19-RAP), the high variability of the CT_{Index} is associated with the practically vertical inclination of the LvsDC. This inclination does not allow to determine the slope easily. In the draining mixture (MDren), the high variability of the CT_{Index} maybe associated with the variation in the value of the curve's total area (which affects the calculation of fracture work). In this mixture, the behavior and tendency of the area under the LvsDC are not consistent and the curve presents different trends between specimens of the same mixture.

To observe that the CT_{Index} provides information which can be complemented with the currently standardized tests, Fig. 11 shows the mean result of the IDT value for each mixture. It is observed that the two mixtures (MDren and MDF-12-ASF), with the best index of tolerance against cracking, now have the lowest performance in the IDT test. In the same way, the mixtures with the lower CT_{Index} (MDC-19-RAP and MDC-12-ASF) have the highest values of indirect tensile strength. Something that stands out is the conventional MDC-19 mixture that remains in the same position. It can even be concluded that, for this reason, it is the most stable and the one that presents the best performance if these two indicators are taken into account (CT_{Index} and IDT).
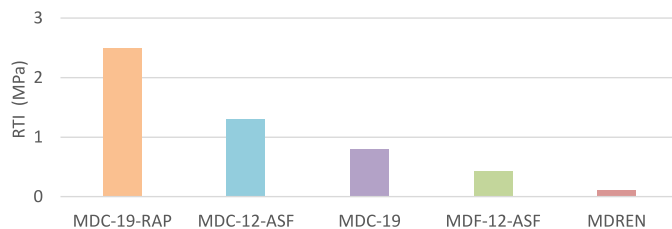

FIG. 11. IDT results of the asphalt mixtures evaluated.

From the IDEAL test applied to different types of asphalt mixtures, it can be observed that:

- Although the MDC-19-RAP mixtures have a high IDT, their fracture tolerance index is low in high concentrations of recycled material. This is due to a sudden failure at 15°C after reaching the maximum load, causing the slope at 75% after the maximum load to be less easily determinable.
- With the MDC-12-ASF mixture, something similar to the RAP mix happens. The natural asphalt binder is an aged asphalt binder, and for this reason, although it does not present a sudden failure, the crack propagation speed for this type of mixtures is high. This can be seen in Fig. 9b.
- The MDC-19 mix presented the best performance, considering the values of CT_{Index} and IDT. This is due to the fact that there is a good relationship between stiffness and ductility. The above is due to its young asphalt binder and dense sieve curve.
- The mixture of natural asphalt binder manufactured in cold (MDF-12-ASF) has the highest CT_{Index}. This is because, as seen in Fig. 9d, it has the highest ductility and less crack propagation speed. Being a cold mixture it does not have high adhesion in its components. The energy that dissipates at the time of maximum load is low and it does not cause a sudden failure. In other words, it is a highly deformable soft mixture.
- The MDREN mixture is a functional mixture of low resistance but high ductility due to its high air voids content and although the implementation of indirect tensile strength test is not for this type of mixtures, the results show a high CT_{Index} and, as it is expected, a low IDT.

Figure 12 presents the result of the acquisition of the examples of surfaces to different asphalt samples. It is observed how MDren and MDC-19 have a greater failure surface compared to the other asphalt mixtures. It is evident that the actual area over which the load performs is not square as it is assumed in the CT_{Index} calculation. Additionally, the theoretical square area assumes a smooth failure plane, but the failure planes due to the fracture of the material present a roughness, which also affects the result. The roughness surface is considered since the resolution of the 3D scanner detects and includes these differences within the area of calculation.

To observe the effect of the fracture area correction in the different mixtures, the graph of the CT_{Index} value calculated for each sample is presented in Fig. 13. The figure shows the result with the square area and the scanned area. Additionally, the relation of areas (corrected area divided by square area) for each test is included in the figure to determine if this correction value is random or stable for each type of asphalt mixture.

From Fig. 13, it is clear that the CT_{Index} calculated with the rectangular area overestimates the samples in the different cases and that the correction area varies significantly from one type of mixture to another. For example, in
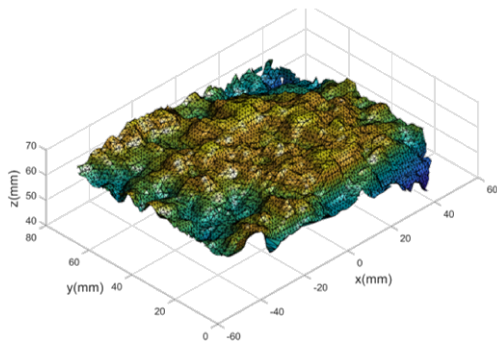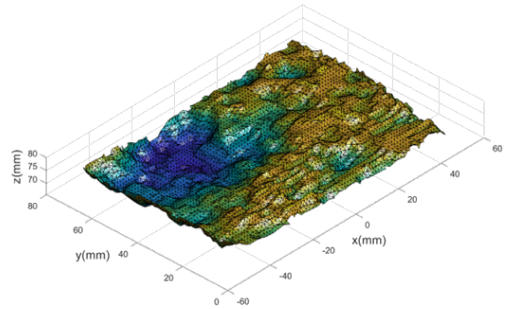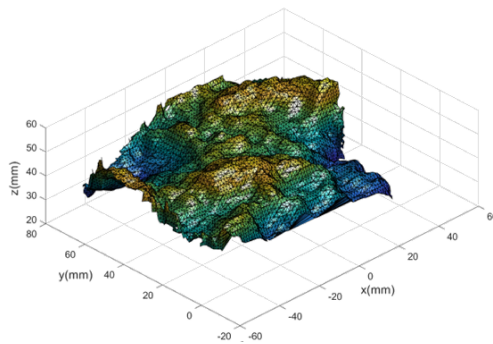
a)
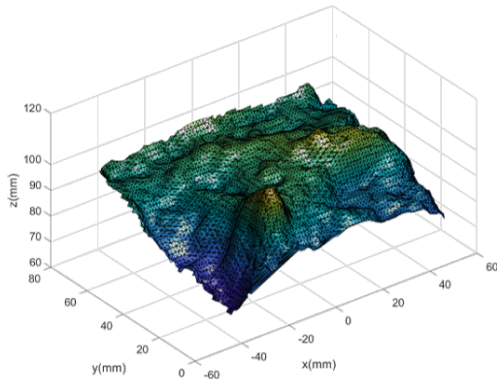
b)
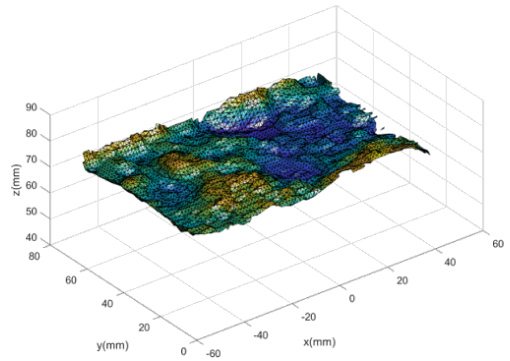
c)

d)

e)

FIG. 12. Example of failure surfaces: a) recycled mix (MDC-19-RAP), b) hot asphaltite mix (MDC-12-ASF), c) dense mix (MDC-19), d) cold asphaltite mix (MDF-12-ASF), and e) draining mix (MDren).

the case of cold asphaltite mix, there is a clear trend and a maximum area correction value of 5%, while the draining mixture has values greater than 23%.
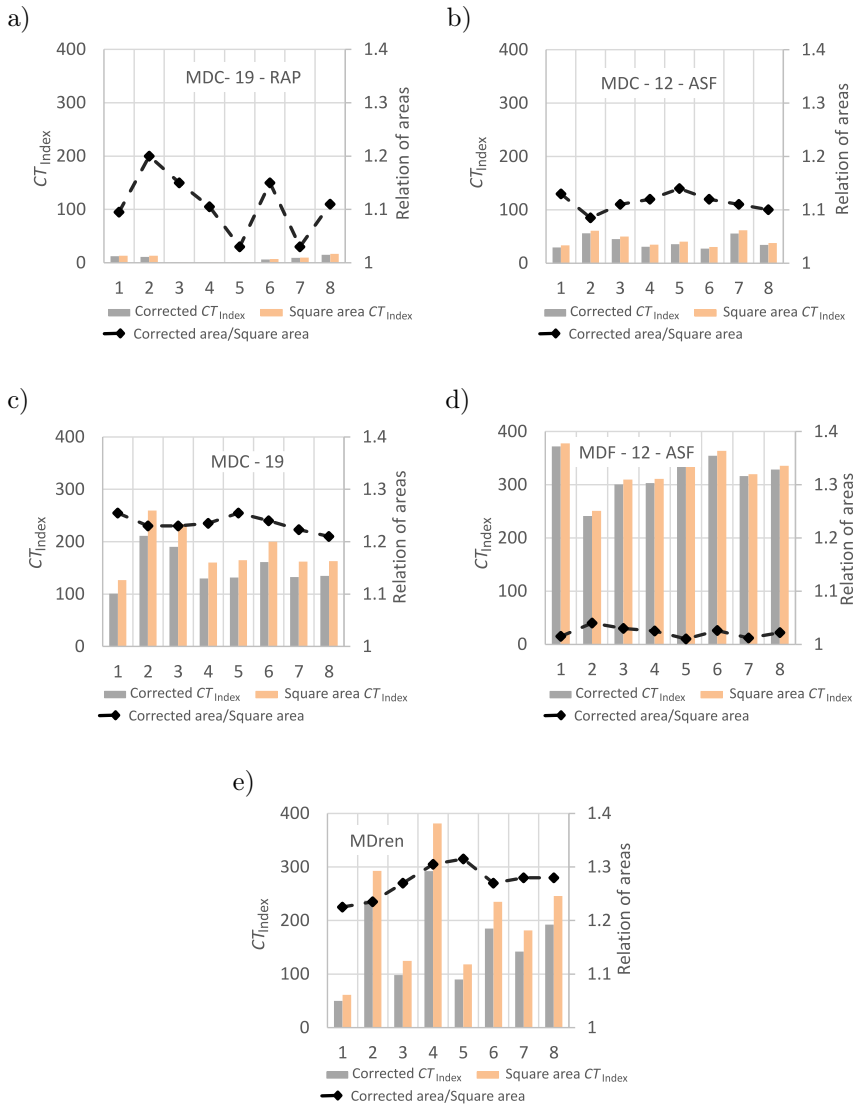
FIG. 13. Crack tolerance index and corrected area values: a) recycled mix (MDC-19-RAP), b) hot asphaltite mix (MDC-12-ASF), c) dense mix (MDC-19), d) cold asphaltite mix (MDF-12-ASF), and e) draining mix (MDren).

The RAP behaves rigidly, and the failure occurs suddenly. The distribution of the RAP failure plane is very heterogeneous among the different samples of the same mixture. This is due to the RAP aggregates, as these have been subjected to previous stresses and weather conditions that have worn away their initial conditions. For this reason, it is observed that MDC-19-RAP mixtures obtain the greatest dispersion in the area correction values.

It is also observed in the results of the CT_{Index} that the MDren and the MDC-19 mixtures have the highest correction index. The fissure in these kinds of mixes generally does not propagate through the center. An explanation of this is that the highest percentage of cracking for MDC-19 is by the sample mastic [25]. In dense or draining mixtures, if the mastic fails, the fissure is propagated along the edge of the aggregate, which in these mixtures is bigger compared to asphaltite mixtures. This produces a failure irregular surface within a greater region. Figure 14 shows the mean of the CT_{Index} and the relation of areas per mixture. The MDren and MDC-19 mixtures have an actual fracture area greater than 20%, compared to the theoretical square area. On the other hand, cold asphaltite (MDF-12-ASF) has a mean of less than 5% due to the low adhesion and cohesion of its materials. This allows the point load to propagate the crack through the middle of the sample without difficulty. Evidence of this is its low resistance (Fig. 7d) compared to the hot natural asphalt mixture.
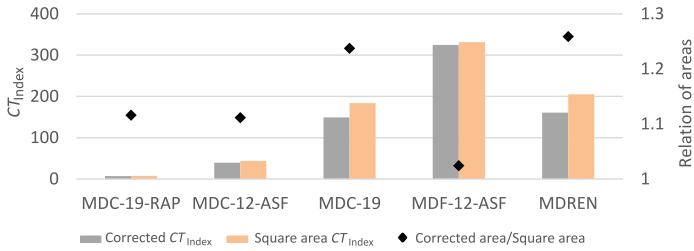

Fig. 14. Tolerance index corrected by type of mixture.

From Fig. 14, it is observed that the CT_{Index} of MDC-19 and MDren without the correction of the area was approximately 40% less than cold asphaltite (MDF-12-ASF). After the correction, it increased to 50%. This shows how the behavior of the mixture is overestimated with the theoretical area. Figure 15 shows the correction factors of the failure area where a correction factor of 1.24, 1.11, and 1.26 are obtained for MDC-19, MDC-12-ASF, and MDren, respectively. The COV for these mixtures is less than 15%, with a clear data trend. Having a reduced range of variation, the values could be taken as correction
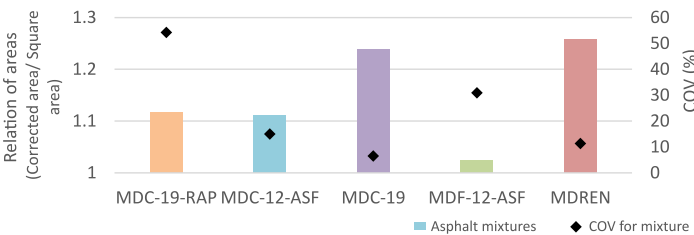

Fig. 15. Area correction factor.

factors for the area in mixtures with this type of material and tested under the same conditions. On the other hand, MDF-12-ASF shows a higher COV of 32%. Although it has an elevated coefficient of variation, the correction of the area less than 5% does not produce a great impact on the results. Thus, the correction is not necessary. The mixture of RAP has a COV of 54%, and the observed data do not show a clear trend (Fig. 13a). Standardizing a correction factor of 1.12 is not recommended under these test conditions. A mixture of 70% RAP or higher increases the heterogeneity of the mixture and better results would not be obtained.

4. Conclusions

The results show that the application of the IDEAL test at 15 °C is feasible for asphalt mixtures with different characteristics such as mixtures modified with RAP, mixtures with different sieve size curves (dense and draining mixtures), and mixtures made with natural asphalt binder compacted hot and cold. The analysis model, in the first place, considers the region of the LvsDC after the failure, since in this region the propagation of the crack can be analyzed. On the other hand, the test procedure is simple since it is the same as for the IDT test, and it is only necessary to capture the entire LvsDC to calculate the CT_{Index}.

The application of the IDEAL test based on the calculation of the CT_{Index} parameter for asphalt mixtures of different types proves to give consistent results for the characterization of the fracture tolerance of conventional dense mixtures and in mixtures manufactured with natural asphalt binder. However, the CT_{Index} calculation showed high dispersion in recycled mixtures (with 70% of RAP) and in draining mixtures at the test conditions presented.

The correction of the area of failure for the IDEAL test is shown to be necessary for some types of mixtures such as dense and draining where the area is 20% higher than what is traditionally taken in a plane form. This percentage, which is not considered, allows an increase in the CT_{Index}, which overestimates the mechanical response of the material studied. The test at different temperatures of a larger number of samples is recommended to limit the correction factor with a higher degree of reliability.

According to the results for the cold asphaltite mixture, the application of the correction factor is not necessary since, with a value of 3%, there is no impact or variation in the calculation of the CT_{Index}. The mixtures manufactured with RAP have a coefficient of variation of 54%, and their tendency is not clear, so it is not possible to obtain a stable correction coefficient due to its sudden fracture. On the other hand, the mixture of hot natural asphalt binder, the dense mixture and the drainage show a COV of the area correction factor less than 20%, so that these can be taken under the same test conditions.

The model developed applies to other types of tests and materials in which the fracture area is an essential variable for the calculation of the resistance or characterization of the materials' mechanical properties. The devices used are low cost and easy accessible. The application of this model in different structures and fields of study is proposed as future work.

Acknowledgments

References

1. Zhou F., Newcomb D., Gurganus Ch., Banihashemrad S., Park E.S., Sakhaeifar M., Lytton R.L., *Final Report of NCHRP 9-57: Experimental Design for Field Validation of Laboratory Tests to Assess Cracking Resistance of Asphalt Mixtures*, Texas A&M Transportation Institute, 2016.

2. Falla G.C., Leischner S., Blasl A, Erlingsson S., Characterization of unbound granular materials within a mechanistic design framework for low volume roads, *Transportation Geotechnics*, **13**: 2–12, 2017, doi: 10.1016/j.trgeo.2017.08.010.

3. Zhou F., *Final Report for NCHRP IDEA Project 195: Development of an IDEAL Cracking Test for Asphalt Mix Design, Quality Control and Quality Assurance*, Texas A&M Transportation Institute, 2019.

4. Lu D.X., Saleh M., Nguyen N.H.T., Effect of rejuvenator and mixing methods on behaviour of warm mix asphalt containing high RAP content, *Construction and Building Materials*, **197**: 792–802, 2019, doi: 10.1016/j.conbuildmat.2018.11.205.

5. Ziari H., Moniri A., Laboratory evaluation of the effect of synthetic Polyolefin-glass fibers on performance properties of hot mix asphalt, *Construction and Building Materials*, **213**: 459–68, 2019, doi: 10.1016/j.conbuildmat.2019.04.084.

6. Pérez-Jiménez F., Botella R., Moon K.-H., Marasteanu M., Effect of load application rate and temperature on the fracture energy of asphalt mixtures. Fénix and semi-circular bending tests, *Construction and Building Materials*, **48**: 1067–1071, 2013, doi: 10.1016/j.conbuildmat.2013.07.084.

7. Mahyuddin A., Tjaronge M.W., Ali N., Isran Ramli M., Experimental analysis on stability and indirect tensile strength in asphalt emulsion mixture containing buton granular asphalt, *International Journal of Applied Engineering Research*, **12**(12): 3162–3169, 2017.

8. Valdés Vidal G., *Evaluation of the cracking process in bituminous mixtures through the development of a new experimental test: Fénix Test* [in Spanish: *Evaluación del proceso de fisuración en las mezclas bituminosas mediante el desarrollo de un nuevo ensayo experimental: Ensayo Fénix*], Ph.D.Thesis, Prog. ITT. Univ. Cataluńa, Barcelona, 2011.

9. Reyes-Ortiz O.J., Alvarez-Lugo A.E., Botella-Nieto R., Study of a hot asphalt mixture response based on energy concepts, *DYNA*, **78**(168): 45–52, 2011.

10. Moaveni M., Cetin S., Brand A.S.., Dahal S., Roesler J.R., Tutumluer E., Machine vision based characterization of particle shape and asphalt coating in Reclaimed Asphalt Pavement, *Transportation Geotechnics*, **6**: 26–37, 2016, doi: 10.1016/j.trgeo.2016.01.001.

11. Tsai B.-W., Coleri E., Harvey J.T., Monismith C.L., Evaluation of AASHTO T 324 Hamburg-Wheel Track Device test, *Construction and Building Materials*, **114**: 248–60, 2016, doi: 10.1016/j.conbuildmat.2016.03.171.

12. Hull D., *Fractography: Observing, Measuring and Interpreting Fracture Surface Topography*, Cambridge University Press, Cambridge, 1999.

13. Reyes-Ortiz O.R., Mejía M., Useche-Castelblanco J.S., Aggregate segmentation of asphaltic mixes using digital image, *Bulletin of the Polish Academy of Sciences: Technical Sciences*, **67**(2): 279–287, 2019, doi: 10.24425/bpas.2019.128115.

14. Reyes Ortiz O.J., Fuentes Pumarejo L.G., Moreno-Torres O.H., Behavior of asphalt mixtures made with wax-modified asphalt [in Spanish: Comportamiento de mezclas asfálticas fabricadas con asfaltos modificados con ceras], *Rev Científica Ing y Desarro*, **31**(1): 161–178, 2013.

15. Inzerillo L., Di Mino G., Roberts R., Image-based 3D reconstruction using traditional and UAV datasets for analysis of road pavement distress, *Automation in Construction*, **96**: 457–469, 2018, doi: 10.1016/j.autcon.2018.10.010.

16. Anderson T.L., *Fracture Mechanics: Fundamentals and Applications*, 4th ed., CRC Press; 2017.

17. Wang L., Ren M., Xing Y., Chen G., Study on affecting factors of interface crack for asphalt mixture based on microstructure, *Construction and Building Materials*, **156**: 1053–1062, 2017, doi: 10.1016/j.conbuildmat.2017.05.160.

18. Stewart C.M., Garcia E., Fatigue crack growth of a hot mix asphalt using digital image correlation, *International Journal of Fatigue*, **120**: 254–266, 2019, doi: 10.1016/j.ijfatigue.2018.11.024.

19. Espinosa L., Wills J., Caro S., Braham A., Influence of the morphology of the cracking zone on the fracture energy of HMA materials, *Materials and Structures*, **52**(2): Article number 35, 2019, doi: 10.1617/s11527-019-1334-0.

20. INVIAS, *Road Construction Specifications and Testing Standards for Road Materials* [in Spanish: *Especificaciones de construcción de carreteras y normas de ensayos para materiales de carreteras*], Inst Nac Vías – Minist Transp, Colombia, 2013.

21. Anochie-Boateng J., Tutumluer E., Characterizing resilient behavior of naturally occurring bituminous sands for road construction, *Journal of Materials in Civil Engineering*, **22**(11): 1085–1092, 2010, doi: 10.1061/(ASCE)MT.1943-5533.0000115.

22. Wang Y., Binaud N., Gogu C., Bes C., Fu J., Determination of Paris' law constants and crack length evolution via Extended and Unscented Kalman filter: An application to aircraft fuselage panels, *Mechanical Systems and Signal Processing*, **80**: 262–281, 2016, doi: 10.1016/j.ymssp.2016.04.027.

23. Papangelo A., Guarino R., Pugno N., Ciavarella M., On unified crack propagation laws, *Engineering Fracture Mechanics*, **207**: 269–276, 2019, doi: 10.1016/j.engfracmech.2018.12.023.

24. Alvarez-Lugo A.E., Reyes-Ortiz O.J., Miró R., A review of the characterization and evaluation of permeable friction cource mixtures [in Spanish: Revisión de la caracterización y evaluación de mezclas drenantes], *Ingeniare. Revista chilena de ingeniería*, **22**(4): 469–482, 2014.

25. Rami K.Z., Amelian S., Kim Y.-R., You T., Little D.N., Modeling the 3D fracture-associated behavior of viscoelastic asphalt mixtures using 2D microstructures, *Engineering Fracture Mechanics*, **182**: 86–99, 2017, doi: 10.1016/j.engfracmech.2017.07.015.